Aging Cell (2014) **13**, pp111–120 Doi: 10.1111/acel.12157

Surface L-type Ca^{2+} channel expression levels are increased in aged hippocampus

Félix Luis Núñez-Santana,[1] Myongsoo Matthew Oh,[1] Marcia Diana Antion,[1] Amy Lee,[2] Johannes Wilhelm Hell[3] and John Francis Disterhoft[1]

[1]Department of Physiology, Feinberg School of Medicine, Northwestern University, Chicago, IL 60611, USA
[2]Departments of Molecular Physiology and Biophysics, Otolaryngology-Head and Neck Surgery, and Neurology, University of Iowa, Iowa City, IA 52242, USA
[3]Department of Pharmacology, University of California, Davis, CA 95615, USA

Summary

Age-related increase in L-type Ca^{2+} channel (LTCC) expression in hippocampal pyramidal neurons has been hypothesized to underlie the increased Ca^{2+} influx and subsequent reduced intrinsic neuronal excitability of these neurons that lead to age-related cognitive deficits. Here, using specific antibodies against $Ca_v1.2$ and $Ca_v1.3$ subunits of LTCCs, we systematically re-examined the expression of these proteins in the hippocampus from young (3 to 4 month old) and aged (30 to 32 month old) F344xBN rats. Western blot analysis of the total expression levels revealed significant reductions in both $Ca_v1.2$ and $Ca_v1.3$ subunits from all three major hippocampal regions of aged rats. Despite the decreases in total expression levels, surface biotinylation experiments revealed significantly higher proportion of expression on the plasma membrane of $Ca_v1.2$ in the CA1 and CA3 regions and of $Ca_v1.3$ in the CA3 region from aged rats. Furthermore, the surface biotinylation results were supported by immunohistochemical analysis that revealed significant increases in $Ca_v1.2$ immunoreactivity in the CA1 and CA3 regions of aged hippocampal pyramidal neurons. In addition, we found a significant increase in the level of phosphorylated $Ca_v1.2$ on the plasma membrane in the dentate gyrus of aged rats. Taken together, our present findings strongly suggest that age-related cognitive deficits cannot be attributed to a global change in L-type channel expression nor to the level of phosphorylation of $Ca_v1.2$ on the plasma membrane of hippocampal neurons. Rather, increased expression and density of LTCCs on the plasma membrane may underlie the age-related increase in L-type Ca^{2+} channel activity in CA1 pyramidal neurons.

Key words: biotinylation; $Ca_v1.2$; $Ca_v1.3$; calcium; phosphorylation; qRT-PCR.

Introduction

The calcium hypothesis of aging (Khachaturian, 1987; Landfield, 1987) posits that age-related cognitive deficits are mainly due to changes in cellular mechanisms that maintain and regulate intracellular Ca^{2+} homeostasis. Among them, change in Ca^{2+} channel number and/or function has been suggested to be a key factor (Khachaturian, 1994). While age-related increase in function of L-type Ca^{2+} channels (LTCCs) in CA1 pyramidal neurons (Moyer & Disterhoft, 1994; Thibault & Landfield, 1996) and rescue of normal aging- and Alzheimer's disease-related cognitive deficits with LTCC antagonists have been demonstrated (Deyo *et al.*, 1989; Ban *et al.*, 1990), there is conflicting evidence for altered number of LTCCs with aging. Increased (Herman *et al.*, 1998; Chen *et al.*, 2000; Veng & Browning, 2002), no change (Blalock *et al.*, 2003; Kadish *et al.*, 2009), and reduced (Rowe *et al.*, 2007) expression levels of the central pore-forming α_1-subunits of the L-type Ca^{2+} channels $Ca_v1.2$ and $Ca_v1.3$ in hippocampus from aged animals have been reported. These apparently conflicting findings may be due to the level of analysis conducted: from single cell to whole hippocampus. Therefore, we systematically examined the expression levels of $Ca_v1.2$ and $Ca_v1.3$ using Western blot, immunohistochemistry, and real-time quantitative PCR analysis in the three major hippocampal regions of young and aged rats.

Results

$Ca_v1.2$ and $Ca_v1.3$ protein levels are reduced in the aged hippocampus

$Ca_v1.2$ and $Ca_v1.3$ expression levels were examined in CA1, CA3, and dentate gyrus (DG) of young ($N = 19$) and aged ($N = 19$) rats using antibodies specific for the two α_1 subunits of these LTCCs (Fig. 1, Fig. S1). We found significantly reduced expression of both $Ca_v1.2$ and $Ca_v1.3$ subunits in all three regions from aged rats (Fig. 2). Furthermore, the reductions were nearly identical for both subunits at each hippocampal region: 40% in CA3, 30% in CA1, and 10–20% in DG as compared with young adults (Fig. 2). Representative full-length blots from Western blot analyses are shown in Fig. S2.

This is the first demonstration that the protein levels of both LTCC α-subunits are reduced throughout the hippocampus of aged rats. However, this raised a conundrum: How can there be increased Ca^{2+} conductance via LTCCs in CA1 pyramidal neurons (Moyer & Disterhoft, 1994; Thibault & Landfield, 1996) with fewer pore-forming subunits? To address this question, we began by examining the level of the $Ca_v1.2$ and $Ca_v1.3$ subunits found on the plasma membrane.

Surface/total ratios of $Ca_v1.2$ and $Ca_v1.3$ are increased in aged hippocampus

We postulated that the relative ratios of $Ca_v1.2$ and/or $Ca_v1.3$ detected on the surface of cell membranes might be elevated in hippocampal tissue from aged rats. To test this hypothesis, we performed cell surface biotinylation assays (Thomas-Crusells *et al.*, 2003) on dorsal hippocampal slices from young ($N = 9$) and aged ($N = 9$) rats.

The surface/total ratio of $Ca_v1.2$ subunit was significantly increased in CA1 (37%) and CA3 (22%) regions of aged rats (Fig. 3A,C). A similar surface/total ratio increase was also observed for the $Ca_v1.3$ subunit, but it was significant only in the CA3 (29%) and not in the CA1 (15%) region of aged rats (Fig. 3B,D).

Correspondence
Dr. John Francis Disterhoft, Department of Physiology, Feinberg School of Medicine, Northwestern University, 303 E. Chicago Ave., Chicago, IL 60611-3008, USA.
Tel.: +(312) 503 7982; fax: +(312) 503 2090;
e-mail: jdisterhoft@northwestern.edu

Accepted for publication *12 August 2013*

Aging Cell

While these results demonstrate that higher levels of LTCCs are present on the cell membrane, they did not provide the location of the increased surface expression. Therefore, we performed immunohistochemical analysis to identify the locus of the increase.

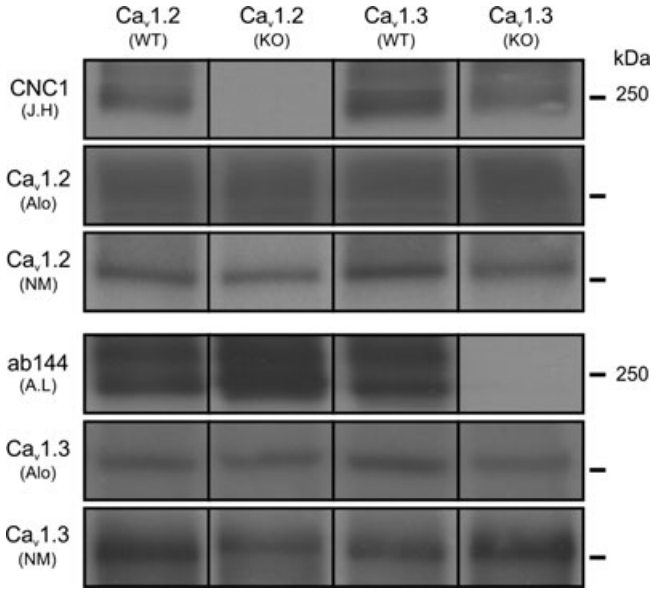

Fig. 1 Characterization of antibody specificity for $Ca_v1.2$ and $Ca_v1.3$ proteins. Hippocampal lysates from wild-type (WT) and L-type-deficient (KO) mice were resolved by SDS-PAGE and immunoblotted with either CNC1 (J.H: Johannes W. Hell), ab144 (A.L: Amy Lee), commercially available anti-$Ca_v1.2$ (Alo: Alomone Labs, ACC-003; NM: Neuromab Antibodies Inc. L57/46,) or commercially available anti-$Ca_v1.3$ (Alo: Alomone Labs, ACC-005; NM: Neuromab Antibodies Inc. N38/8) antibodies. Blots were developed using Amersham ECL Plus and Hyperfilm ECL. Both anti-$Ca_v1.2$ and anti-$Ca_v1.3$ antibodies from commercial sources revealed nonspecific bands in hippocampal lysates from KO tissue. CNC1 and ab144 showed no cross-reactivity with either $Ca_v1.3$ or $Ca_v1.2$ proteins in hippocampal lysates. Note that this example figure is assembled from multiple blots with similar exposure time that have been aligned for illustrative purposes only. See Fig. S1 for immunoblots as loaded in gel.

$Ca_v1.2$ immunoreactivity ($Ca_v1.2$-IR) is increased in somatic region of aged CA1 and CA3 neurons

CA1 pyramidal neurons from aged subjects have been shown to have increased LTCC activity (Thibault & Landfield, 1996) and enhanced calcium action potentials (Moyer & Disterhoft, 1994). Therefore, we postulated that increases in LTCC subunit expression would be observed mostly in the somatic region of aged CA1 pyramidal neurons.

We observed $Ca_v1.2$-IR within the hippocampal formation and hippocampal cell layers similar to previous reports (Hell *et al.*, 1993; Clark *et al.*, 2003; Hall *et al.*, 2013). Significant increases in $Ca_v1.2$-IR were observed in the somatic regions of aged CA1 (Fig. 4) and CA3 (Fig. 5) pyramidal neurons. No change in $Ca_v1.2$-IR and expression was observed in DG granule cells (Fig. 6). Furthermore, no significant changes in $Ca_v1.2$ subunit expression were observed in stratum radiatum of CA1 (Fig. 4C) or CA3 (Fig. 5C) hippocampal region.

In addition, as LTCCs are found in glial cells and its expression has been documented to change with astrocyte activation after brain injury, trauma, and aging (Wisniewski & Terry, 1973; Vaughan & Peters, 1974; MacVicar, 1984; Westenbroek *et al.*, 1998; Chung *et al.*, 2001; Djamshidian *et al.*, 2002; Finch, 2003; Xu *et al.*, 2007), we also examined whether the observed plasma membrane increases in LTCC subunits with aging were of glial/astrocytic origin. No detectable expression/colocalization of LTCC subunits was observed in glial cells with our antibodies (Figs 4–6).

Parallel to $Ca_v1.2$, immunohistochemical experiments were conducted to assess changes in $Ca_v1.3$ protein expression at the cellular level. However, the presence of various nonspecific, high-intensity bands in our $Ca_v1.3$ Western blots (Fig. S2B,D) prevents us from confidently reporting our $Ca_v1.3$ immunohistochemical findings, as the obtained $Ca_v1.3$ immunoreactivity might be the results of nonspecific binding of our current antibody in brain tissue. Hence, it remains to be determined whether immunohistochemical analyses of $Ca_v1.3$ expression at the cellular level are consistent with our $Ca_v1.3$ biotinylation experiments.

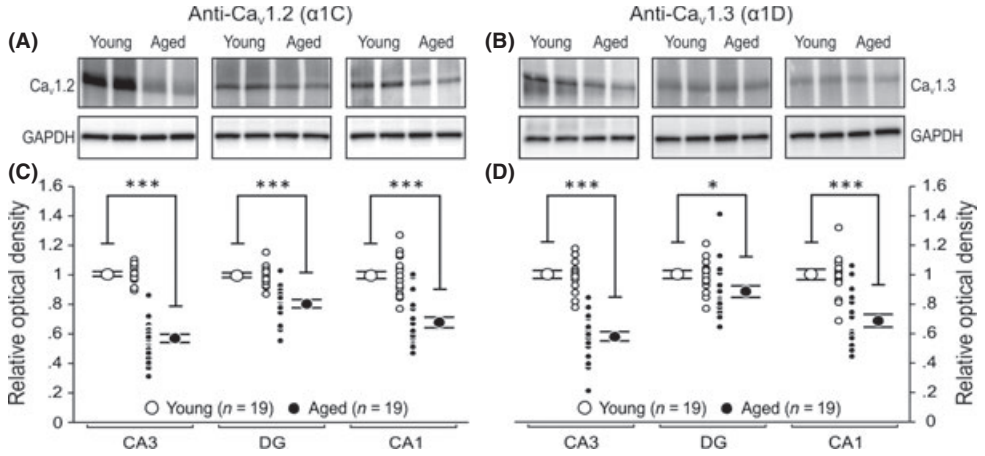

Fig. 2 Total $Ca_v1.2$ and $Ca_v1.3$ L-type calcium channel protein levels are reduced in all three major hippocampal regions of aged rats. Homogenates from whole CA3, DG, and CA1 of dorsal hippocampus (four 1-mm-thick slices per animal) were analyzed using semi-quantitative Western blotting techniques and immunoblotted using highly specific antibodies against $Ca_v1.2$ and $Ca_v1.3$ L-type calcium channel α_1 subunits. (A, B) Representative Western blots comparing expression of $Ca_v1.2$ and $Ca_v1.3$ proteins in CA3, DG, and CA1 regions from two young and two aged rats. Young and aged CA3, DG, and CA1 region samples were resolved in pairs (side by side) on the same gel. Note that a shorter exposure time was used for DG region for the purpose of illustration (See Figs S2 and S5). (C, D) Quantitation of total L-type calcium channel expression normalized to GAPDH and relative to young for each region. All results were confirmed by repeating the experiments and analysis three times. Significant reductions in $Ca_v1.2$ and $Ca_v1.3$ were observed in all three major hippocampal regions of aged animals. Unpaired *t*-test: $*P < 0.05$, $***P < 0.0001$. Data reported as the mean ± SEM.

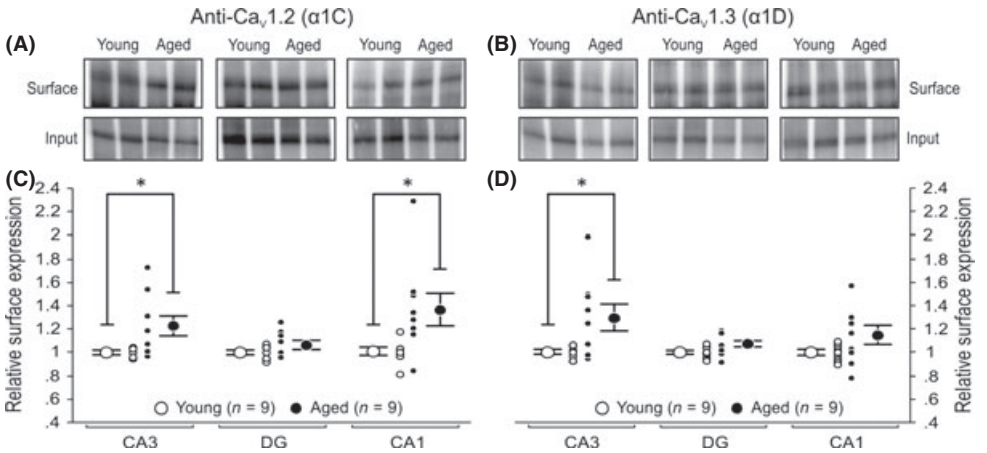

Fig. 3 Age-related increases in the ratio of $Ca_V1.2$ and $Ca_V1.3$ proteins found on the plasma membrane as compared with the total protein levels found in specific regions of the hippocampus. Eight 250 μm thick acute hippocampal slices from 9 young and 9 aged rats were randomly selected and exposed to Sulfo-NHS–SS–biotin-labeling reagent before cell surface proteins were isolated using streptavidin magnetic beads. Control assays with biotinylated lysate proteins were also carried out to verify successful isolation of plasma membrane proteins in all three regions. We found little to no detection of our internal control protein, GAPDH, on surface fractions (See Fig. S3). (A, B) Representative Western blots comparing expression of $Ca_V1.2$ and $Ca_V1.3$ proteins in plasma membrane of CA3, DG, and CA1 from two young and two aged rats. Young and aged CA3, DG, and CA1 region samples were resolved in pairs (side by side) on the same gel. Note that a shorter exposure time was used for DG region for the purpose of illustration (See Figs S2 and S5). (C, D) Quantitation of surface L-type calcium channel protein expression normalized to young. (C) Ratio of surface-to-total expression of $Ca_V1.2$ protein was found to be significantly higher in regions CA1 and CA3 of aged hippocampus. (D) Age-related increase in $Ca_V1.3$ surface-to-total expression was only observed in the CA3 region. All results were confirmed by repeating the experiments and analysis twice. Unpaired *t*-test: $*P < 0.05$. Data reported as the mean ± SEM.

Phosphorylation of surface-expressed $Ca_V1.2$ is increased in the DG of aged rats

Increased LTCC activity by 4-6-fold has been reported when the $Ca_V1.2$ subunits are phosphorylated (Sculptoreanu *et al.*, 1993; Kavalali *et al.*, 1997). In addition, Serine 1928 (S1928) (Davare & Hell, 2003) and Serine 1700 (S1700) (Fuller *et al.*, 2010) of $Ca_V1.2$ can be phosphorylated, but only S1928 phosphorylation has been shown to be increased with normal aging (Davare & Hell, 2003). Therefore, we further explored the possibility that more S1928 in $Ca_V1.2$ might be phosphorylated in the hippocampal regions from aged rats. Biotinylated plasma membrane proteins were isolated and immunoblotted with anti-CH1923-1932P (p1928), an antibody designed to specifically detect $Ca_V1.2$ when phosphorylated at S1928 (De Jongh *et al.*, 1996; Davare & Hell, 2003). We found a significant 1.18-fold increase in phosphorylated $Ca_V1.2$ in DG of aged rats (Fig. 7B). No significant age-related difference in phosphorylated $Ca_V1.2$ was detected in either CA1 or CA3.

$Ca_V1.2$ and $Ca_V1.3$ mRNA levels are unchanged with aging

A positive correlation between $Ca_V1.3$ mRNA and LTCC activity has been previously demonstrated in CA1 pyramidal neurons using single cell reverse transcription PCR experiments (Chen *et al.*, 2000). Therefore, we performed a systematic assay to assess $Ca_V1.2$ and $Ca_V1.3$ mRNA levels in each hippocampal region using the real-time quantitative PCR method to determine whether the mRNA levels were altered with normal aging and/or in a specific hippocampal region(s). We found no significant age-related changes in mRNA levels for both $Ca_V1.2$ and $Ca_V1.3$ (Table 1, Fig. S4).

Discussion

The present study is the first to demonstrate that the pore-forming α_1 subunits for the L-type voltage-gated Ca^{2+} channels ($Ca_V1.2$ and $Ca_V1.3$) are significantly reduced in whole tissue lysates from all three major hippocampal regions of aged rats (Fig. 2). However, the biotinylation and immunohistochemical data demonstrate that age-related increases in $Ca_V1.2$ are observed in CA1 and CA3 regions. Notably, the increase in the $Ca_V1.2$ subunit was in the somatic region of CA1 and CA3 pyramidal neurons (Figs 4 and 5). In addition, no detectable expression/colocalization of $Ca_V1.2$ subunits was observed in glial cells with our antibodies (Figs 4–6). Therefore, the present results support the 'calcium hypothesis of aging' (Khachaturian, 1987; Landfield, 1987) in that the age-related increase in surface expression of L-type voltage-gated Ca^{2+} channels ($Ca_V1.2$ and $Ca_V1.3$) in hippocampal pyramidal neurons we demonstrate may play an important role in the cognitive deficits observed in normal aging subjects.

Phosphorylation of $Ca_V1.2$ LTCC has been previously shown to enhance Ca^{2+} influx (Sculptoreanu *et al.*, 1993; Kavalali *et al.*, 1997). $Ca_V1.2$ α_1 subunit can be phosphorylated at Serine 1928 (S1928) (Davare & Hell, 2003) and at Serine 1700 (S1700) (Fuller *et al.*, 2010), and it has been suggested that S1700 phosphorylation plays a greater modulatory role than S1928 phosphorylation (Brandmayr *et al.*, 2012). However, only S1928 phosphorylation has been shown to be increased in the hippocampus with normal aging (Davare & Hell, 2003). Similarly, we also found significant age-related increase in S1928 phosphorylation, but only in the DG with no apparent changes in other hippocampal regions (Fig. 7). The difference with the previous report (Davare & Hell, 2003) may be due to our focus on the phosphorylation of cell surface channels in each hippocampal region of the dorsal hippocampus, whereas the previous report examined S1928 phosphorylation in the entire hippocampus. In addition, we found high level of $Ca_V1.2$ protein in the DG as compared with CA1 and CA3 from whole tissue lysate (Fig. S5). Furthermore, no age-related changes in the Ca^{2+}-dependent postburst afterhyperpolarization have been observed in DG granule cells (Baskys *et al.*, 1987; Niesen *et al.*, 1988; Reynolds & Carlen, 1989). Therefore, S1928 phosphorylation cannot account for increased calcium influx and reduced neuronal excitability with normal

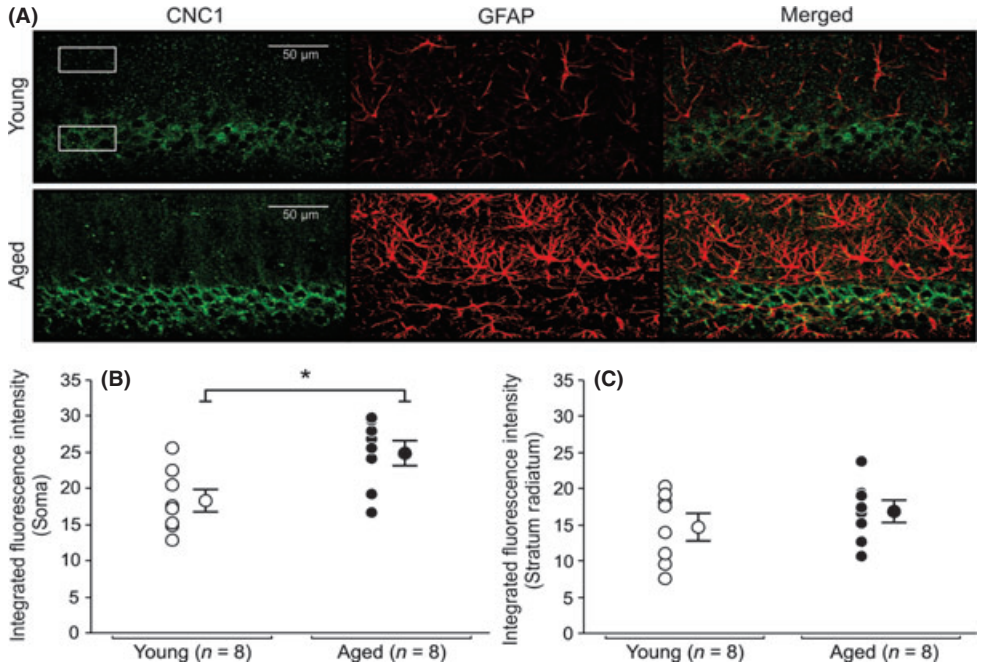

Fig. 4 Expression of $Ca_v1.2$ L-type subunit in soma and radiatum of young and aged CA1 pyramidal neurons. (A) Representative confocal images of hippocampal CA1 pyramidal layer sections showing immunohistochemical labeling for $Ca_v1.2$ (CNC1) of a young and an aged rat. Six regions of interest (box) with equal dimensions in both the stratum pyramidale (3) and the stratum radiatum (3) layers of CA1 were drawn to collect immunofluorescence data. (B) Quantitative analysis of integrated fluorescence intensity in soma of CA1 pyramidal neurons of young and aged rats. (C) Quantitative analysis of integrated fluorescence intensity in the stratum radiatum of young and aged rats. Significant increases in somatic expression of $Ca_v1.2$ subunit were observed in aged CA1 pyramidal neurons (B) ($P < 0.05$). No significant differences in $Ca_v1.2$ subunit expression were detected between stratum radiatum of young and aged rats. No colocalization of CNC1 was observed in glial cells. AutoQuant image deconvolution software (Media Cybernetics, Rockville, MD) was used to reduce background signal for the purpose of illustration. Fluorescence intensities and analyses were performed using raw, unmodified, images. Data reported as the mean ± SEM.

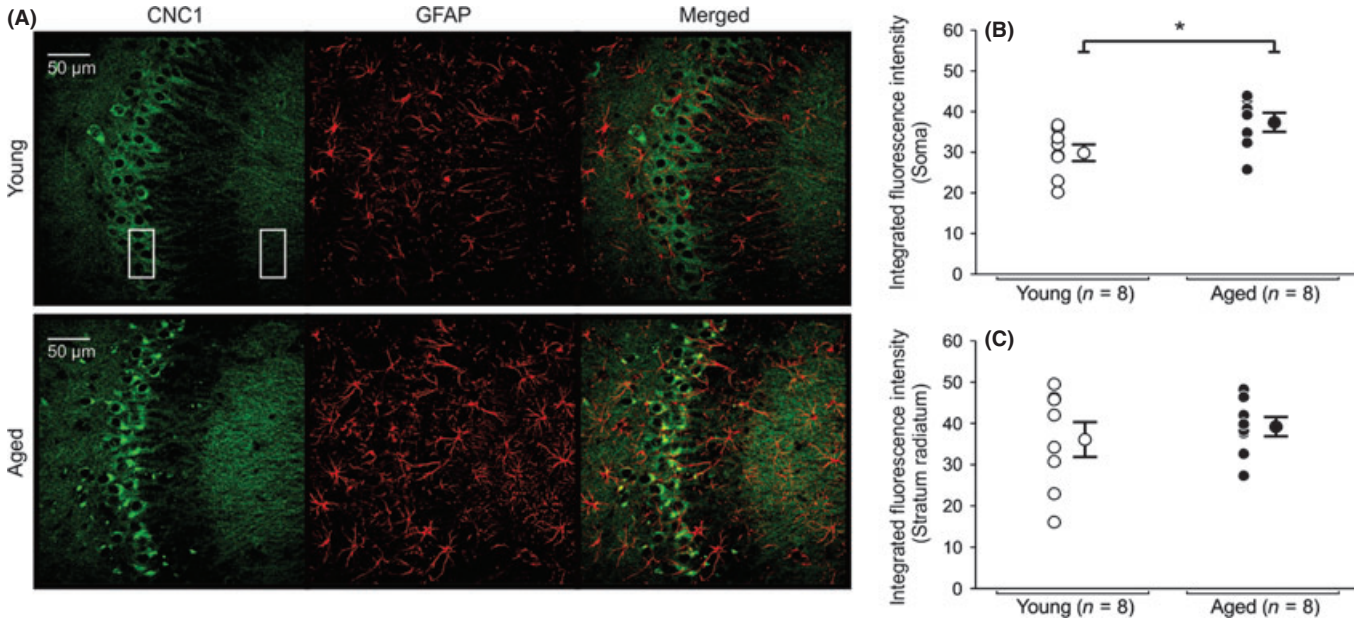

Fig. 5 Expression of $Ca_v1.2$ L-type subunit in soma and radiatum of young and aged CA3 pyramidal neurons. (A) Representative confocal images of hippocampal CA3 pyramidal layer sections showing immunohistochemical labeling for $Ca_v1.2$ (CNC1) of a young and an aged rat. Six regions of interest (box) with equal dimensions in both the stratum pyramidale (3) and the stratum radiatum (3) layers of CA3 were drawn to collect immunofluorescence data. (B) Quantitative analysis of integrated fluorescence intensity in soma of CA3 pyramidal neurons of young and aged rats. (C) Quantitative analysis of integrated fluorescence intensity in the stratum radiatum of young and aged rats. Significant increases in somatic expression of $Ca_v1.2$ subunit were observed in aged CA3 pyramidal neurons (B) ($P < 0.05$). No significant differences in $Ca_v1.2$ subunit expression were detected between stratum radiatum of young and aged rats. No colocalization of CNC1 was observed in glial cells. AutoQuant image deconvolution software (Media Cybernetics, Rockville, MD) was used to reduce background signal for the purpose of illustration. Fluorescence intensities and analyses were performed using raw, unmodified, images. Data reported as the mean ± SEM.

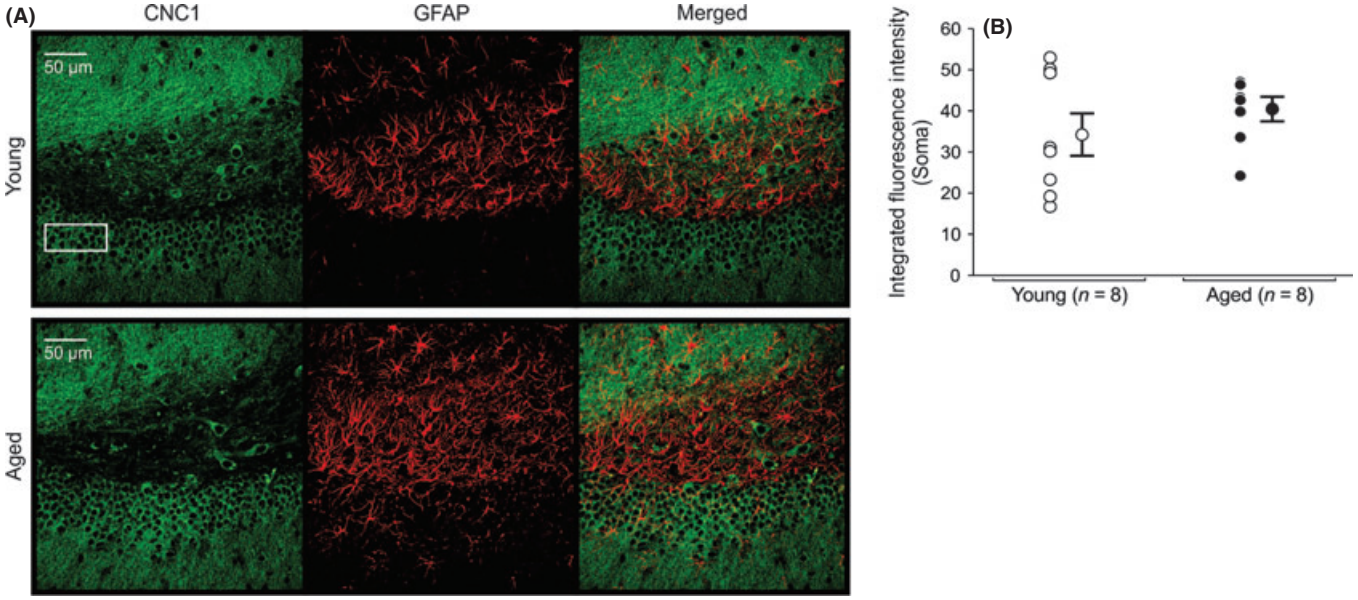

Fig. 6 Expression of $Ca_v1.2$ L-type subunit in DG granular cells of young and aged hippocampus. (A) Representative confocal images of hippocampal DG granular cells showing immunohistochemical labeling for $Ca_v1.2$ (CNC1) of a young and an aged rat. Three regions of interest placed atop the granular layer were drawn to collect immunofluorescence data. (B) Quantitative analysis of integrated fluorescence intensity of granular cells in DG of young and aged rats. No significant differences in $Ca_v1.2$ subunit expression were detected in granular cells of young and aged rats. No colocalization of CNC1 was observed in glial cells. AutoQuant image deconvolution software (Media Cybernetics, Rockville, MD) was used to reduce background signal for the purpose of illustration. Fluorescence intensities and analyses were performed using raw, unmodified, images. Data reported as the mean ± SEM.

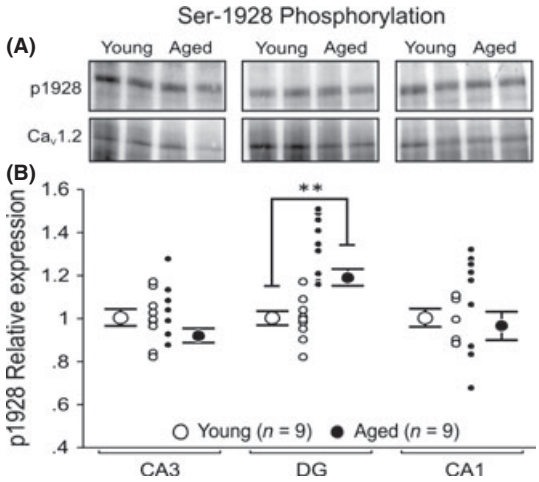

Fig. 7 Phosphorylation of Serine 1928 is significantly increased in cell surface-expressed $Ca_v1.2$ proteins in DG of aged rat. Biotinylated CA1, CA3, and DG cell surface fractions were resolved and immunoblotted with p1928 and CNC1 antibody to determine the relative expression of phosphorylated $Ca_v1.2$ proteins localized at the cell membrane. The relative level of phosphorylation of Serine 1928 on $Ca_v1.2$ protein was determined by normalizing the obtained p1928 signals to the corresponding CNC1 signals for the loaded surface fraction. (A) Representative Western blots comparing cell surface expression of p1928 and $Ca_v1.2$ protein in CA3, DG, and CA1 from two young and two aged rats. (B) Quantitation of p1928 with relation to total cell surface-expressed $Ca_v1.2$ protein in young and aged rats. We found no significant age-related differences in phosphorylation of $Ca_V1.2$ on CA1 or CA3 region. However, a significant increase in phosphorylation was observed on DG region of aged rats. All results were confirmed by repeating the experiments and analysis twice. Unpaired *t*-test: $^{**}P < 0.005$. Data reported as the mean ± SEM.

aging observed in CA1 hippocampal pyramidal neurons (Landfield & Pitler, 1984; Moyer *et al.*, 1992; Moyer & Disterhoft, 1994; Thibault & Landfield, 1996).

We found no age-related changes in $Ca_v1.2$ or $Ca_v1.3$ mRNA expression in the present study. Previous reports examining the mRNA or LTCC α-subunits in hippocampus from aged animals have been inconsistent; with groups reporting an increase (Herman *et al.*, 1998; Chen *et al.*, 2000; Veng & Browning, 2002), no change (Blalock *et al.*, 2003; Kadish *et al.*, 2009), or reductions (Rowe *et al.*, 2007) in mRNA or α-subunit expression with aging. The discrepancy between the findings may be due to the anatomical specificity and/or method of analysis used in the studies (i.e. differences in splice variants amplified by the different primers of different groups). At single cell resolution, a positive correlation between $Ca_v1.3$ mRNA levels and functional channel density in the adult and aged CA1 pyramidal neurons has been reported: that is, the more $Ca_v1.3$ mRNA, the greater the LTCC activity (Chen *et al.*, 2000). Using whole hippocampus, a report using semi-quantitative RNAse protection analysis revealed that $Ca_v1.2$ and $Ca_v1.3$ mRNA expression levels are increased in aged rats (Herman *et al.*, 1998), whereas no change in either mRNA (Blalock *et al.*, 2003; Kadish *et al.*, 2009) or a reduction in $Ca_v1.2$ mRNA (Rowe *et al.*, 2007) were reported using microarray methods. Our present real-time quantitative PCR data support the lack of change in $Ca_v1.2$ or $Ca_v1.3$ mRNA expression level with normal aging in the subregions of the hippocampus (Table 1). Notably, we also observed that the level of $Ca_v1.2$ and $Ca_v1.3$ mRNA expressions was different than that for the protein levels: for protein, DG > CA3 ≥ CA1 (Fig. S5): for mRNA, CA3 ≥ CA1 > DG (Table 1). Furthermore, a 4-fold increase in $Ca_v1.2$ mRNA relative to $Ca_v1.3$ mRNA was observed in the CA1 region, which supports the previous reports that approximately 80% of LTCCs are $Ca_v1.2$ channels (Hell *et al.*, 1993; Clark *et al.*, 2003).

The exact mechanism by which LTCC activity is increased with aging in CA1 neurons is as yet unclear. While our findings provide a better understanding of the processes that take place during aging, we cannot exclude the role that other processes may have in channel function, activity, and intracellular Ca^{2+} concentrations. For example, the activity of the pore-forming LTCC α-subunits can be regulated by

Table 1 L-type calcium channel mRNA levels within the hippocampal subregions are not altered by normal aging

	CA1		CA3		DG	
	ΔC_T^{YOUNG}	ΔC_T^{OLD}	ΔC_T^{YOUNG}	ΔC_T^{OLD}	ΔC_T^{YOUNG}	ΔC_T^{OLD}
$Ca_v1.2$ RT-PCR						
Pair 1	5.66	5.66	4.94	5.15	6.72	7.02
Pair 2	5.68	5.30	5.04	5.10	7.15	6.96
Pair 3	5.54	5.34	4.79	4.68	6.68	7.02
Pair 4	5.44	5.73	4.86	5.20	7.05	7.27
Pair 5	5.85	5.52	5.02	4.90	6.92	6.73
Pair 6	5.69	5.90	4.95	4.73	7.03	6.80
Pair 7	5.64	5.38	4.84	4.69	6.78	6.92
Average ± SD	5.64 ± 0.13	5.55 ± 0.22	4.92 ± 0.09	4.92 ± 0.23	6.90 ± 0.18	6.96 ± 0.17
$\Delta\Delta C_T$ ($\Delta C_T^{OLD} - \Delta C_T^{YOUNG}$)		−0.10 ± 0.26		0.00 ± 0.25		0.06 ± 0.25
Fold change ($2^{-\Delta\Delta C}$T)		1.07		1.00		0.96
$Ca_v1.3$ RT-PCR						
Pair 1	7.29	7.30	5.78	5.91	6.76	7.19
Pair 2	7.10	6.96	5.78	5.77	7.14	7.44
Pair 3	7.13	7.12	5.54	5.59	7.10	7.49
Pair 4	6.85	7.25	5.59	5.91	7.24	7.19
Pair 5	7.30	7.05	5.89	5.75	7.06	6.96
Pair 6	7.42	7.30	5.56	5.57	7.22	7.20
Pair 7	7.06	6.78	5.63	5.53	7.32	7.39
Average ± SD	7.16 ± 0.19	7.11 ± 0.19	5.68 ± 0.13	5.72 ± 0.16	7.12 ± 0.18	7.27 ± 0.18
$\Delta\Delta C_T$ ($\Delta C_T^{OLD} - \Delta C_T^{Y0UNG}$)		−0.05 ± 0.27		0.04 ± 0.21		0.15 ± 0.26
Fold change ($2^{-\Delta\Delta C}$T)		1.04		0.98		0.96

Total RNA was isolated from major hippocampal regions of young and aged rats. Equivalent amounts were converted into cDNA. Real-time quantitative PCR was performed on triplicates of subject for $Ca_v1.2$, $Ca_v1.3$, and GAPDH. ΔC_T is calculated by subtracting threshold fluorescence of internal housekeeping gene GAPDH, for example, ($C_T^{CaV1.2} - C_T^{Gapdh}$).

protein–protein interactions, a number of which can enhance L-type channel function (Catterall, 2000; Calin-Jageman & Lee, 2008). Second, calcineurin expression levels and activity have also been shown to be increased in hippocampus from aged animals (Foster *et al.*, 2001; Norris *et al.*, 2005; Eto *et al.*, 2008) and inhibiting it reduces LTCC activity (Norris *et al.*, 2002, 2010) and the Ca^{2+}-dependent postburst afterhyperpolarization (AHP) (Vogalis *et al.*, 2004). Third, post-translational modifications of the $Ca_v1.2$ LTCC protein by proteolytic cleavage of the C-terminus region can significantly impact voltage-dependent activation and activity of the channel (Wei *et al.*, 1994; Hulme *et al.*, 2006). Finally, $Ca_v1.2$ and $Ca_v1.3$ channels are regulated by proteosomal degradation (Altier *et al.*, 2011; Gregory *et al.*, 2011) and oxidative stress through the action of reactive oxygen species, which can lead to increased accumulation of Ca^{2+} inside hippocampal neurons. (Kourie, 1998; Fusi *et al.*, 2001).

Age-related increase in LTCC function, specifically in CA1 pyramidal neurons, has been a popular hypothesis to explain age-related cognitive deficits (Disterhoft & Oh, 2006; Foster, 2007; Thibault *et al.*, 2007). Previous reports have demonstrated that Ca^{2+} influx into neurons is significantly increased in CA1 pyramidal neurons from aged animals (Moyer & Disterhoft, 1994; Thibault & Landfield, 1996) due to increased density of LTCCs (Thibault & Landfield, 1996), which leads to reduced intrinsic excitability (Landfield & Pitler, 1984; Thompson *et al.*, 1990; Moyer *et al.*, 1992) and synaptic plasticity (Norris *et al.*, 1998). Rescue of age-related cognitive deficits (Deyo *et al.*, 1989) and restoration of intrinsic neuronal excitability (Moyer *et al.*, 1992; Norris *et al.*, 1998) and synaptic plasticity (Norris *et al.*, 1998) with the use of LTCC blockers (e.g. nimodipine and nifedipine) have further provided support for the previously held viewpoint. In addition to the enhanced Ca^{2+} influx via LTCCs, Ca^{2+} released from the endoplasmic reticulum through ryanodine receptors via the Ca^{2+}-induced Ca^{2+}-release (CICR) mechanism has been suggested and shown to greatly reduce excitability (i.e., increase postburst AHP) of CA1 pyramidal neurons from aged rats (Kumar & Foster, 2004; Gant *et al.*, 2006; Kim *et al.*, 2007; Thibault *et al.*, 2007). Therefore, while increased LTCC function is a significant source of the age-related cognitive deficits, other sources of Ca^{2+} that are changed with normal aging should also be systematically characterized.

The increased LTCC surface expression was not observed in all of the aged rats examined (Figs 3–5). This heterogeneity was expected as we have previously reported that nearly half of the aged cohort of 27–31-month-old F344xBN rats are learning-impaired (Knuttinen *et al.*, 2001; Matthews *et al.*, 2009). Similar age-related heterogeneity has been reported for other strains of rats (Gallagher *et al.*, 1993; Tombaugh *et al.*, 2005) and in rabbits (Thompson *et al.*, 1996; Moyer *et al.*, 2000). More importantly, it has been demonstrated that learning-impaired aged animals have CA1 pyramidal neurons with enlarged postburst AHP (Moyer *et al.*, 2000; Tombaugh *et al.*, 2005; Matthews *et al.*, 2009). Therefore, we hypothesize that only those aged subjects with increased surface expression of functional LTCCs are likely to be cognitively impaired given the contribution of Ca^{2+} influx via L-type Ca^{2+} channels to the AHP. Additional studies are required to determine whether such correlation exists.

In summary, our results suggest that age-related cognitive deficits cannot be attributed to a global change in L-type Ca^{2+} channel expression or to the level of phosphorylation of $Ca_v1.2$ channels in the plasma membrane of aged hippocampal neurons. Rather, we provide evidence that age-related increases in plasma membrane expression and/or distribution of L-type Ca^{2+} channels in the somatic regions of CA1 and CA3 pyramidal neurons may underlie the reported changes in neuronal excitability and activity observed with normal aging.

Materials and methods

Subjects

Young adults (3–4 month old) and aged (30–32 month old) male F1 hybrid Fischer 344 X Brown Norway rats (F344xBN; Harlan, Indianapolis, IN, USA) were used in this study. Rats were group housed with ad libitum access to food and water and maintained in a climate-controlled room with a 14:10 h light/dark cycle. The F344xBN rats are long-lived with > 50% survival rate at 34 months of age (National Institute on Aging, Aged Rodent Colonies Handbook, www.nia.nih.gov/research/dab/aged-rodent-colonies-handbook/ strain-survival-information) and have significantly less pathological complications with normal aging as compared with the Fischer 344 (F344) rats (Bronson, 1990; Lipman *et al.*, 1996). Every effort was made to ensure that only healthy rats were included in the experiments. Rats with palpable tumors, skin ulcerations, infections, or difficulty moving were excluded from the studies. All experimental procedures were approved by the Northwestern University Animal Care and Use Committee and conformed to NIH standards (NIH Publications No. 80-23). All efforts were made to minimize animals' discomfort and the number of animals used.

For CNC1 antibody specificity, brains and cerebellar tissue from conditional knockout mice with a forebrain-specific (hippocampus and forebrain) deletion of $Ca_v1.2$ were used (McKinney *et al.*, 2008; White *et al.*, 2008). For ab144 antibody specificity, brains from knockout mice with a global deletion of the gene encoding $Ca_v1.3$ were used (Platzer *et al.*, 2000; Clark *et al.*, 2003; McKinney & Murphy, 2006). Tissue from knockout mice and their wild-type littermates were generously provided by Dr. Geoffrey G. Murphy (University of Michigan, Ann Arbor, MI, USA).

Antibodies

The previously characterized rabbit anti-$Ca_v1.2$ (CNC1) antibody (provided by J.W. Hell) was raised against a peptide covering residues 818 – 835 within the cytoplasmic loop between domains II and III of the $Ca_v1.2$ protein (Hell *et al.*, 1993; Hall *et al.*, 2013). The rabbit anti-$Ca_v1.3$ (Ab144) antibody (provided by A. Lee) was raised against a synthetic peptide corresponding to $Ca_v1.3$ N-terminal sequence (MQHQRQQQED-HANEANYARGTRKC; Covance Research Products, Denver, PA, USA) (Jenkins *et al.*, 2010; Gregory *et al.*, 2011). Specificity is further demonstrated in Fig. S1. The rabbit anti-CH1923-1932P (p1928) antibody, which specifically binds to phosphorylated $Ca_v1.2$ when phosphorylated at Serine 1928, was raised against a phosphopeptide consisting of residues 1923–1932 (De Jongh *et al.*, 1996; Davare & Hell, 2003). Rabbit polyclonal antiglyceraldehyde-3-phosphate dehydrogenase (GAPDH) antibody was obtained from Abcam (Cambridge, MA, USA) and chicken anti-glial fibrillary acidic protein (GFAP) antibody was obtained from Millipore (Temecula, CA, USA).

Sample preparation and Immunoblotting

Whole dorsal hippocampi from 19 young and 19 aged rats were dissected out and immediately placed in cold (approximately 0 °C) oxygenated (95%/5% O_2/CO_2) aCSF (in mM: 124 NaCl, 1.25 NaH_2PO_4, 2.5 KCl, 26 $NaHCO_3$, 25 glucose, 2.4 $CaCl_2$, and 2.0 $MgSO_4$, pH 7.4) before transverse dorsal hippocampal slices (400 μm) were made using a manual tissue slicer (Stoelting Co., Wood Dale, IL, USA). The hippocampal slices were then transferred to fresh oxygenated ice-cold aCSF containing several protease and phosphatase inhibitors (1 μg mL^{-1} pepstatin A, 10 μg mL^{-1} leupeptin, 20 μg mL^{-1} aprotinin, 200 nM phenylmethanesulfonyl fluoride, 8 μg mL^{-1} calpain inhibitor I, 8 μg mL^{-1} calpain inhibitor II, 1 mM *p*-nitrophenyl phosphate, 50 mM NaF, 20 mM sodium pyrophosphate, and 4 μM microcystin LR) and immediately microdissected under a microscope (Zeiss Stemi DV4) to yield the three major hippocampal subdivisions (CA1, CA3, and Dentate Gyrus) (Coultrap *et al.*, 2005). Each microdissected region was individually homogenized and sonicated in 1% Triton X-100 lysis buffer containing protease and phosphatase inhibitors and cleared by ultracentrifugation. Protein concentration was determined by the BCA assay using bovine serum albumin (BSA) as a standard (Pierce, Rockford, IL, USA).

For quantification of total L-type Ca^{2+} channel expression in the three major hippocampal regions of young and aged rats, samples containing equal amounts of proteins (20 μg) were resolved by SDS-PAGE and analyzed by immunoblotting with either anti-CNC1 or Ab144. Fresh blots were used for each channel of interest, and each blot was reprobed with GAPDH for normalization and to control for variability during sample loading. Immunoreactive bands were visualized using a Chem-iDoc XRS+ Molecular Imager System with Image Lab™ Software (Bio-Rad Laboratories, Hercules, CA, USA), and only signals doubling with increasing exposure times were used for quantification and analysis. All immunoblots were measured and quantified by densitometry using NIH IMAGEJ image analysis software (rsb.info.nih.gov/ij/).

Whole slice cell surface biotinylation

To assess the relative cell surface expression of L-type Ca^{2+} channels in hippocampal pyramidal neurons, cell surface biotinylation experiments were conducted on acute hippocampal slices (n = 8, 250 μm slices per rat) from nine young and nine aged rats. This technique has been successfully shown to reach all layers of acute hippocampal slices of up to 400 μm in thickness using Sulfo-NHS–SS–biotin as labeling reagent with very low to no labeling of intracellular proteins (Thomas-Crusells *et al.*, 2003). Alternate slices from the dorsal half of both left and right hippocampi were exposed to 1 mg mL^{-1} Sulfo-NHS–SS–biotin-labeling reagent (Pierce) for 30 min before separating each hippocampal region for processing and isolation of surface proteins using streptavidin magnetic beads (Pierce).

Immunoblotting with p1928, CNC1, and Ab144 antibody was performed after SDS-PAGE separation of total region lysates (input) and biotinylated (surface) fraction proteins. GAPDH was used as both loading and internal protein control to confirm the success of the biotinylation procedures (Fig. S3).

L-type Ca^{2+} channel surface expression and phosphorylation of $Ca_v1.2$ measurements

Following Western blot analysis, optical density values for total lysate (input) and biotinylated (surface) fractions were obtained and the relative ratio of surface expression for each subunit was determined by normalizing the surface optical density value to its corresponding input band density value. The level of phosphorylation of Serine 1928 on $Ca_v1.2$ protein was determined by normalizing the obtained p1928 band to the total CNC1 intensity for the loaded surface fraction. To quantify the level of p1928 phosphorylation of surface-expressed $Ca_v1.2$ channels, blots were initially probed with p1928, stripped, and reprobed with CNC1 antibody.

RNA isolation and cDNA synthesis

CA1, CA3, and DG regions were isolated from young and aged rats in pairs, homogenized in RPLT-Plus Lysis Buffer (Qiagen, Valencia, CA, USA)

and stored at −80 °C until RNA isolation. Samples were further dissociated with QiaShredder columns, and the total RNA was isolated via Qiagen RNEasy Plus Kit according to manufacturer's directions. RNA was dissolved into 60 μl RNAse-free water, stored on ice, and the yield was determined with a nanodrop spectrophotometer (Thermo-Scientific, Rockford, IL, USA). 650 ng (CA1, CA3) or 240 ng (DG) of total RNA was converted into cDNA with reverse transcriptase and multiple primers (qScript™ cDNA SuperMix; Quanta Biosciences, Gaithersburg, MD, USA) on a thermocycler per manufacturer's instructions and stored at −20 °C until use. Synthesis of cDNA was commenced within 2 h of RNA isolation.

Immunohistochemistry

Young (3–4 month old) and aged (30–32 month old) male F344xBN rats were anesthetized and intracardially perfused with ice-cold sodium phosphate buffer (0.1 M PB [pH 7.4]) supplemented with several protease and phosphatase inhibitors (PPI; cOmplete and PhosSTOP Inhibitor Cocktail Tablets; Roche, Indianapolis, IN, USA) and followed by ice-cold 4% paraformaldehyde in PB (supplemented with PPI). Brains were removed, postfixed (overnight), and cryoprotected by successively sinking in 10% (w/v) and 30% (w/v) sucrose in PB at 4 °C for 72 h (Marshall *et al.*, 2011). Forty-micrometer-thick coronal sections containing the hippocampus were made, hippocampus dissected out, and stored at −20 °C in cryoprotectant solution (0.1 M PBS, pH 7.4, 30% (w/v) sucrose, 30% (v/v) ethylene glycol and 1% (w/v) polyvinylpyrrolidone) (Watson *et al.*, 1986) until processed for immunohistochemistry.

Immunohistochemistry (IHC) was performed as previously described (Ferraguti *et al.*, 2004; Wu *et al.*, 2008) with some modifications. The tissue processing and data collection and analysis were performed blind to the age of the animals. Five hippocampal slices from each animal were systemically and randomly selected for double immunolabeling with antibodies against glial fibrillary acidic protein (GFAP) and $Ca_v1.2$ or $Ca_v1.3$. The free-floating sections were rinsed in 0.1 M Dulbecco's phosphate-buffered saline (DPBS) for 30 min to remove cryoprotectant, incubated with 0.05% boric acid in DPBS for 10 min, rinsed in DPBS containing 0.1% Tween-20 (DPBS-T) for 30 min, and blocked in DPBS containing 5% normal donkey serum, 1% immunoglobulin- and protease-free bovine serum albumin, and 0.3% Triton X-100 for 2 h. The sections were then incubated in chicken anti-GFAP (diluted 1:500) and anti-$Ca_v1.2$ (CNC1; diluted 1:500) or anti-$Ca_v1.3$ (ab144; diluted 1:2000) overnight at 4 °C, rinsed in DPBS-T for 30 min, incubated in FITC-conjugated secondary antibody against rabbit IgG (diluted 1:500) and Texas Red-conjugated secondary antibody against chicken IgG (diluted 1:500) (Jackson immunoresearch, West Grove, PA) for 1 h at room temperature, rinsed in DPBS-T for 1 h, rinsed in DPBS for 10 min, and finally mounted and coverslipped using ProLong® Gold antifade reagent with DAPI (Molecular Probes, Eugene, OR, USA). Control hippocampal sections from young and aged rats were also included in the assay and treated the same way, but either the primary, secondary, or both antibodies were excluded from the incubating solution. All slices from young and aged animals were simultaneously processed during the experiment in order to minimize the effects of potential inter-batch staining variability.

Image analysis

Confocal images from CA1 region of hippocampus were obtained at a magnification of 40× using a Nikon Eclipse C1si Spectral Imaging Confocal Microscope System at the Nikon Imaging Center and Cell Imaging Facility at Northwestern University. Exposure parameters for $Ca_v1.2$, $Ca_v1.3$, and GFAP were standardized across all captured images and maintained throughout image acquisition for both young and aged hippocampal slides. Images were analyzed using MetaMorph® imaging software (Molecular Devices, Sunnyvale, CA, USA), and statistical analyses were performed using StatView software. To study age-related changes in L-type subunit expression in CA1 and CA3, data were collected from raw, unmodified, images by drawing three rectangular regions of interest (ROI) with equal dimensions in both the stratum pyramidale and the stratum radiatum layers of CA1 and CA3 regions. For DG, ROIs were placed atop the granular cell layer. The fluorescence intensity for each ROI was then averaged to calculate the integrated fluorescent intensity for each hippocampal slice. Averaged values from all 5 hippocampal slices from each animal were then averaged to collect the animal's integrated fluorescent intensity used for plotting and statistical analysis. Significant group differences in protein expression were evaluated using analysis of variance (ANOVA) with statistical significance set to $P < 0.05$. All data are reported as the means ± SEM.

Real-time PCR of mRNA levels

Primer sequences compatible with rat and mouse were a gift from C. Savio Chan (Northwestern University). The primers were designed to bridge exons of cDNA to eliminate concern of genomic DNA contamination and previously tested for comparable efficiency during PCR. Primers include Cacna1c, bridging exons 7–8 [sense primer-GGCATCACCAACTTCGACA, antisense Primer- TACACCCAGGGCAACTCATA], Cacna1d, bridging exons 41–42 [sense primer-TGACATTGGGCCAGAAATCC, antisense primer- GGTGGTATTGGTCTGCTGAA], and GAPDH, bridging exons 3–4 [sense primer- GCTGAGTATGTCGTGGAGTCTA, antisense primer-TTCTCGTGGTTCACACCCAT]. For real-time quantitative PCR, 1 pair of young and aged cDNA (1 μL) triplicate samples from each of CA1, CA3, and DG were measured in parallel for threshold fluorescence accumulation (C_T) of each gene target (Cacna1c, Cacna1d, and GAPDH) in a 96-well tray with a Step One Plus™ Applied Biosystems QPCR Machine using SYBR Green as a reporter and ROX™ dye as a passive reference control. After PCR, a melt curve analysis was done for each sample to ensure that the primers were specific. The threshold C_T was manually set to be 1.1 ΔRn (reporter-reference control baseline fluorescence) for all targets and fell within the exponential phase of amplification. The comparative $\Delta\Delta C_T$ method described by Livak and Schmittgen (Livak & Schmittgen, 2001) was used to compare young and aged samples with GAPDH, which was used as internal housekeeping control. ΔC_T for each sample target gene was calculated as follows: $\Delta C_T = (\text{mean } C_T^{\text{Target}} - \text{mean } C_T^{\text{Gapdh}})$. To obtain fold change due to age, $\Delta\Delta C_T$ was calculated with the following equation: $(\Delta C_T^{\text{AGED}} - \Delta C_T^{\text{Young}})$ and presented in Table 1.

Statistical analysis

All statistical analyses were performed using STATVIEW analysis software, and significant group differences in protein expression were evaluated using analysis of variance (ANOVA) with statistical significance set to $P < 0.05$. All data are reported as the mean ± SEM. Duplicates were performed on all reported phosphorylation and surface expression assays.

Acknowledgments

The authors thank Dr. Geoffrey G. Murphy (University of Michigan, Ann Arbor. MI.) for generously providing us with $Ca_v1.2$ and $Ca_v1.3$ KO

tissue; Dr C. Savio Chan and Vivian Hernandez for technical assistance, reagents, and use of real-time PCR equipment; Drs. Johannes W. Hell and Amy Lee for their contributions to conceptual discussions and practical input; Drs. Geoffrey T. Swanson, Bryan A. Copits, and Jeffrey Burgdorf for discussions regarding biotinylation experiments; Drs. Murali Prakriya, Robert Vassar, and Peter Penzes for valuable discussions during the study, and Dr. Dina Simkin for critical review of the manuscript. Immunohistochemical data were collected and analyzed at the Northwestern University Cell Imaging Facility generously supported by NCI CCSG P30 CA060553 awarded to the Robert H Lurie Comprehensive Cancer Center. This work was supported by National Institutes of Health Grants AG008796 (J.F.D), AG017139 (J.F.D.), AG017502 (J.W.H.), DC009433 (A.L), and HL087120 (A.L.), and a Carver Research Program of Excellence Award (A.L.).

Author contributions

F.L.N., M.M.O. and J.F.D. designed research; F.L.N. and M.D.A. performed research; F.L.N. and M.D.A. analyzed data; J.W.H. and A.L. contributed reagents; M.M.O., F.L.N. and J.F.D. drafted the manuscript; All authors wrote/edited the paper.

Conflict of interest

None.

References

Altier C, Garcia-Caballero A, Simms B, You H, Chen L, Walcher J, Tedford HW, Hermosilla T, Zamponi GW (2011) The Cavbeta subunit prevents RFP2-mediated ubiquitination and proteasomal degradation of L-type channels. *Nat. Neurosci.* **14**, 173–180.

Ban TA, Morey L, Aguglia E, Azzarelli O, Balsano F, Marigliano V, Caglieris N, Sterlicchio M, Capurso A, Tomasi NA, Crepaldi G, Volpe D, Palmieri G, Ambrosi G, Polli E, Cortellaro M, Zanussi C, Froldi M (1990) Nimodipine in the treatment of old age dementias. *Prog. Neuropsychopharmacol. Biol. Psychiatry* **14**, 525–551.

Baskys A, Niesen CE, Carlen PL (1987) Altered modulatory actions of serotonin on dentate granule cells of aged rats. *Brain Res.* **419**, 112–118.

Blalock EM, Chen KC, Sharrow K, Herman JP, Porter NM, Foster TC, Landfield PW (2003) Gene microarrays in hippocampal aging: statistical profiling identifies novel processes correlated with cognitive impairment. *J. Neurosci.* **23**, 3807–3819.

Brandmayr J, Poomvanicha M, Domes K, Ding J, Blaich A, Wegener JW, Moosmang S, Hofmann F (2012) Deletion of the C-terminal phosphorylation sites in the cardiac beta-subunit does not affect the basic beta-adrenergic response of the heart and the Ca(v)1.2 channel. *J. Biol. Chem.* **287**, 22584–22592.

Bronson RT (1990) *Genetic Effects of Aging II*. Caldwell, NJ: Telford Press.

Calin-Jageman I, Lee A (2008) Ca(v)1 L-type Ca2+ channel signaling complexes in neurons. *J. Neurochem.* **105**, 573–583.

Catterall WA (2000) Structure and regulation of voltage-gated Ca2+ channels. *Annu. Rev. Cell Dev. Biol.* **16**, 521–555.

Chen KC, Blalock EM, Thibault O, Kaminker P, Landfield PW (2000) Expression of alpha 1D subunit mRNA is correlated with L-type Ca2+ channel activity in single neurons of hippocampal "zipper" slices. *Proc. Natl Acad. Sci. USA* **97**, 4357–4362.

Chung YH, Shin CM, Kim MJ, Cha CI (2001) Enhanced expression of L-type Ca2+ channels in reactive astrocytes after ischemic injury in rats. *Neurosci. Lett.* **302**, 93–96.

Clark NC, Nagano N, Kuenzi FM, Jarolimek W, Huber I, Walter D, Wietzorrek G, Boyce S, Kullmann DM, Striessnig J, Seabrook GR (2003) Neurological phenotype and synaptic function in mice lacking the CaV1.3 alpha subunit of neuronal L-type voltage-dependent Ca2+ channels. *Neuroscience* **120**, 435–442.

Coultrap SJ, Nixon KM, Alvestad RM, Valenzuela CF, Browning MD (2005) Differential expression of NMDA receptor subunits and splice variants among the CA1, CA3 and dentate gyrus of the adult rat. *Brain Res. Mol. Brain Res.* **135**, 104–111.

Davare MA, Hell JW (2003) Increased phosphorylation of the neuronal L-type Ca (2+) channel Ca(v)1.2 during aging. *Proc. Natl Acad. Sci. USA* **100**, 16018–16023.

De Jongh KS, Murphy BJ, Colvin AA, Hell JW, Takahashi M, Catterall WA (1996) Specific phosphorylation of a site in the full-length form of the alpha 1 subunit of the cardiac L-type calcium channel by adenosine 3′,5′-cyclic monophosphate-dependent protein kinase. *Biochemistry* **35**, 10392–10402.

Deyo RA, Straube KT, Disterhoft JF (1989) Nimodipine facilitates associative learning in aging rabbits. *Science* **243**, 809–811.

Disterhoft JF, Oh MM (2006) Learning, aging and intrinsic neuronal plasticity. *Trends Neurosci.* **29**, 587–599.

Djamshidian A, Grassl R, Seltenhammer M, Czech T, Baumgartner C, Schmidbauer M, Ulrich W, Zimprich F (2002) Altered expression of voltage-dependent calcium channel alpha(1) subunits in temporal lobe epilepsy with Ammon's horn sclerosis. *Neuroscience* **111**, 57–69.

Eto R, Abe M, Hayakawa N, Kato H, Araki T (2008) Age-related changes of calcineurin and Akt1/protein kinase Balpha (Akt1/PKBalpha) immunoreactivity in the mouse hippocampal CA1 sector: an immunohistochemical study. *Metab. Brain Dis.* **23**, 399–409.

Ferraguti F, Cobden P, Pollard M, Cope D, Shigemoto R, Watanabe M, Somogyi P (2004) Immunolocalization of metabotropic glutamate receptor 1alpha (mGluR1alpha) in distinct classes of interneuron in the CA1 region of the rat hippocampus. *Hippocampus* **14**, 193–215.

Finch CE (2003) Neurons, glia, and plasticity in normal brain aging. *Neurobiol. Aging* **24**(Suppl. 1), S123–S127; discussion S131.

Foster TC (2007) Calcium homeostasis and modulation of synaptic plasticity in the aged brain. *Aging Cell* **6**, 319–325.

Foster TC, Sharrow KM, Masse JR, Norris CM, Kumar A (2001) Calcineurin links Ca2+ dysregulation with brain aging. *J. Neurosci.* **21**, 4066–4073.

Fuller MD, Emrick MA, Sadilek M, Scheuer T, Catterall WA (2010) Molecular mechanism of calcium channel regulation in the fight-or-flight response. *Sci. Signal.* **3**, ra 70.

Fusi F, Saponara S, Gagov H, Sgaragli G (2001) 2,5-Di-t-butyl-1,4-benzohydroquinone (BHQ) inhibits vascular L-type Ca(2+) channel via superoxide anion generation. *Br. J. Pharmacol.* **133**, 988–996.

Gallagher M, Burwell R, Burchinal M (1993) Severity of spatial learning impairment in aging: development of a learning index for performance in the Morris water maze. *Behav. Neurosci.* **107**, 618–626.

Gant JC, Sama MM, Landfield PW, Thibault O (2006) Early and simultaneous emergence of multiple hippocampal biomarkers of aging is mediated by Ca2+ -induced Ca2+ release. *J. Neurosci.* **26**, 3482–3490.

Gregory FD, Bryan KE, Pangrsic T, Calin-Jageman IE, Moser T, Lee A (2011) Harmonin inhibits presynaptic Cav1.3 Ca(2)(+) channels in mouse inner hair cells. *Nat. Neurosci.* **14**, 1109–1111.

Hall DD, Dai S, Tseng PY, Malik Z, Nguyen M, Matt L, Schnizler K, Shephard A, Mohapatra DP, Tsuruta F, Dolmetsch RE, Christel CJ, Lee A, Burette A, Weinberg RJ, Hell JW (2013) Competition between alpha-actinin and Ca(2+)-calmodulin controls surface retention of the L-type Ca(2+) channel CaV1.2. *Neuron* **78**, 483–497.

Hell JW, Westenbroek RE, Warner C, Ahlijanian MK, Prystay W, Gilbert MM, Snutch TP, Catterall WA (1993) Identification and differential subcellular localization of the neuronal class C and class D L-type calcium channel alpha 1 subunits. *J. Cell Biol.* **123**, 949–962.

Herman JP, Chen KC, Booze R, Landfield PW (1998) Up-regulation of alpha1D Ca2+ channel subunit mRNA expression in the hippocampus of aged F344 rats. *Neurobiol. Aging* **19**, 581–587.

Hulme JT, Yarov-Yarovoy V, Lin TW, Scheuer T, Catterall WA (2006) Autoinhibitory control of the CaV1.2 channel by its proteolytically processed distal C-terminal domain. *J. Physiol.* **576**, 87–102.

Jenkins MA, Christel CJ, Jiao Y, Abiria S, Kim KY, Usachev YM, Obermair GJ, Colbran RJ, Lee A (2010) Ca2+ -dependent facilitation of Cav1.3 Ca2+ channels by densin and Ca2+ /calmodulin-dependent protein kinase II. *J. Neurosci.* **30**, 5125–5135.

Kadish I, Thibault O, Blalock EM, Chen KC, Gant JC, Porter NM, Landfield PW (2009) Hippocampal and cognitive aging across the lifespan: a bioenergetic shift precedes and increased cholesterol trafficking parallels memory impairment. *J. Neurosci.* **29**, 1805–1816.

Kavalali ET, Hwang KS, Plummer MR (1997) cAMP-dependent enhancement of dihydropyridine-sensitive calcium channel availability in hippocampal neurons. *J. Neurosci.* **17**, 5334–5348.

Khachaturian ZS (1987) Hypothesis on the regulation of cytosol calcium concentration and the aging brain. *Neurobiol. Aging* **8**, 345–346.
Khachaturian ZS (1994) Calcium hypothesis of Alzheimer's disease and brain aging. *Ann. N. Y. Acad. Sci.* **747**, 1–11.
Kim S, Yun HM, Baik JH, Chung KC, Nah SY, Rhim H (2007) Functional interaction of neuronal Cav1.3 L-type calcium channel with ryanodine receptor type 2 in the rat hippocampus. *J. Biol. Chem.* **282**, 32877–32889.
Knuttinen MG, Gamelli AE, Weiss C, Power JM, Disterhoft JF (2001) Age-related effects on eyeblink conditioning in the F344 x BN F1 hybrid rat. *Neurobiol. Aging* **22**, 1–8.
Kourie JI (1998) Interaction of reactive oxygen species with ion transport mechanisms. *Am. J. Physiol.* **275**, C1–C24.
Kumar A, Foster TC (2004) Enhanced long-term potentiation during aging is masked by processes involving intracellular calcium stores. *J. Neurophysiol.* **91**, 2437–2444.
Landfield PW (1987) 'Increased calcium-current' hypothesis of brain aging. *Neurobiol. Aging* **8**, 346–347.
Landfield PW, Pitler TA (1984) Prolonged Ca2+ -dependent afterhyperpolarizations in hippocampal neurons of aged rats. *Science* **226**, 1089–1092.
Lipman RD, Chrisp CE, Hazzard DG, Bronson RT (1996) Pathologic characterization of brown Norway, brown Norway x Fischer 344, and Fischer 344 x brown Norway rats with relation to age. *J. Gerontol. A Biol. Sci. Med. Sci.* **51**, B54–B59.
Livak KJ, Schmittgen TD (2001) Analysis of relative gene expression data using real-time quantitative PCR and the 2(-Delta Delta C(T)) Method. *Methods* **25**, 402–408.
MacVicar BA (1984) Voltage-dependent calcium channels in glial cells. *Science* **226**, 1345–1347.
Marshall MR, Clark JP III, Westenbroek R, Yu FH, Scheuer T, Catterall WA (2011) Functional roles of a C-terminal signaling complex of CaV1 channels and A-kinase anchoring protein 15 in brain neurons. *J. Biol. Chem.* **286**, 12627–12639.
Matthews EA, Linardakis JM, Disterhoft JF (2009) The fast and slow afterhyperpolarizations are differentially modulated in hippocampal neurons by aging and learning. *J. Neurosci.* **29**, 4750–4755.
McKinney BC, Murphy GG (2006) The L-Type voltage-gated calcium channel Cav1.3 mediates consolidation, but not extinction, of contextually conditioned fear in mice. *Learn. Mem.* **13**, 584–589.
McKinney BC, Sze W, White JA, Murphy GG (2008) L-type voltage-gated calcium channels in conditioned fear: a genetic and pharmacological analysis. *Learn. Mem.* **15**, 326–334.
Moyer JR Jr, Disterhoft JF (1994) Nimodipine decreases calcium action potentials in rabbit hippocampal CA1 neurons in an age-dependent and concentration-dependent manner. *Hippocampus* **4**, 11–17.
Moyer JR Jr, Thompson LT, Black JP, Disterhoft JF (1992) Nimodipine increases excitability of rabbit CA1 pyramidal neurons in an age- and concentration-dependent manner. *J. Neurophysiol.* **68**, 2100–2109.
Moyer JR Jr, Power JM, Thompson LT, Disterhoft JF (2000) Increased excitability of aged rabbit CA1 neurons after trace eyeblink conditioning. *J. Neurosci.* **20**, 5476–5482.
Niesen CE, Baskys A, Carlen PL (1988) Reversed ethanol effects on potassium conductances in aged hippocampal dentate granule neurons. *Brain Res.* **445**, 137–141.
Norris CM, Halpain S, Foster TC (1998) Reversal of age-related alterations in synaptic plasticity by blockade of L-type Ca2+ channels. *J. Neurosci.* **18**, 3171–3179.
Norris CM, Blalock EM, Chen KC, Porter NM, Landfield PW (2002) Calcineurin enhances L-type Ca(2+) channel activity in hippocampal neurons: increased effect with age in culture. *Neuroscience* **110**, 213–225.
Norris CM, Kadish I, Blalock EM, Chen KC, Thibault V, Porter NM, Landfield PW, Kraner SD (2005) Calcineurin triggers reactive/inflammatory processes in astrocytes and is upregulated in aging and Alzheimer's models. *J. Neurosci.* **25**, 4649–4658.
Norris CM, Blalock EM, Chen KC, Porter NM, Thibault O, Kraner SD, Landfield PW (2010) Hippocampal 'zipper' slice studies reveal a necessary role for calcineurin in the increased activity of L-type Ca(2+) channels with aging. *Neurobiol. Aging* **31**, 328–338.
Platzer J, Engel J, Schrott-Fischer A, Stephan K, Bova S, Chen H, Zheng H, Striessnig J (2000) Congenital deafness and sinoatrial node dysfunction in mice lacking class D L-type Ca2+ channels. *Cell* **102**, 89–97.
Reynolds JN, Carlen PL (1989) The effects of midazolam on hippocampal dentate gyrus granule neurons from young and old Fischer 344 rats. *Can. J. Physiol. Pharmacol.* **67**, 359–362.
Rowe WB, Blalock EM, Chen KC, Kadish I, Wang D, Barrett JE, Thibault O, Porter NM, Rose GM, Landfield PW (2007) Hippocampal expression analyses reveal selective association of immediate-early, neuroenergetic, and myelinogenic pathways with cognitive impairment in aged rats. *J. Neurosci.* **27**, 3098–3110.
Sculptoreanu A, Rotman E, Takahashi M, Scheuer T, Catterall WA (1993) Voltage-dependent potentiation of the activity of cardiac L-type calcium channel alpha 1 subunits due to phosphorylation by cAMP-dependent protein kinase. *Proc. Natl Acad. Sci. USA* **90**, 10135–10139.
Thibault O, Landfield PW (1996) Increase in single L-type calcium channels in hippocampal neurons during aging. *Science* **272**, 1017–1020.
Thibault O, Gant JC, Landfield PW (2007) Expansion of the calcium hypothesis of brain aging and Alzheimer's disease: minding the store. *Aging Cell* **6**, 307–317.
Thomas-Crusells J, Vieira A, Saarma M, Rivera C (2003) A novel method for monitoring surface membrane trafficking on hippocampal acute slice preparation. *J. Neurosci. Methods* **125**, 159–166.
Thompson LT, Deyo RA, Disterhoft JF (1990) Nimodipine enhances spontaneous activity of hippocampal pyramidal neurons in aging rabbits at a dose that facilitates associative learning. *Brain Res.* **535**, 119–130.
Thompson LT, Moyer JR Jr, Disterhoft JF (1996) Trace eyeblink conditioning in rabbits demonstrates heterogeneity of learning ability both between and within age groups. *Neurobiol. Aging* **17**, 619–629.
Tombaugh GC, Rowe WB, Rose GM (2005) The slow afterhyperpolarization in hippocampal CA1 neurons covaries with spatial learning ability in aged Fisher 344 rats. *J. Neurosci.* **25**, 2609–2616.
Vaughan DW, Peters A (1974) Neuroglial cells in the cerebral cortex of rats from young adulthood to old age: an electron microscope study. *J. Neurocytol.* **3**, 405–429.
Veng LM, Browning MD (2002) Regionally selective alterations in expression of the alpha(1D) subunit (Ca(v)1.3) of L-type calcium channels in the hippocampus of aged rats. *Brain Res. Mol. Brain Res.* **107**, 120–127.
Vogalis F, Harvey JR, Furness JB (2004) Suppression of a slow post-spike afterhyperpolarization by calcineurin inhibitors. *Eur. J. Neurosci.* **19**, 2650–2658.
Watson RE Jr, Wiegand SJ, Clough RW, Hoffman GE (1986) Use of cryoprotectant to maintain long-term peptide immunoreactivity and tissue morphology. *Peptides* **7**, 155–159.
Wei X, Neely A, Lacerda AE, Olcese R, Stefani E, Perez-Reyes E, Birnbaumer L (1994) Modification of Ca2+ channel activity by deletions at the carboxyl terminus of the cardiac alpha 1 subunit. *J. Biol. Chem.* **269**, 1635–1640.
Westenbroek RE, Bausch SB, Lin RC, Franck JE, Noebels JL, Catterall WA (1998) Upregulation of L-type Ca2+ channels in reactive astrocytes after brain injury, hypomyelination, and ischemia. *J. Neurosci.* **18**, 2321–2334.
White JA, McKinney BC, John MC, Powers PA, Kamp TJ, Murphy GG (2008) Conditional forebrain deletion of the L-type calcium channel Ca V 1.2 disrupts remote spatial memories in mice. *Learn. Mem.* **15**, 1–5.
Wisniewski HM, Terry RD (1973) Morphology of the aging brain, human and animal. *Prog. Brain Res.* **40**, 167–186.
Wu WW, Chan CS, Surmeier DJ, Disterhoft JF (2008) Coupling of L-type Ca2+ channels to KV7/KCNQ channels creates a novel, activity-dependent, homeostatic intrinsic plasticity. *J. Neurophysiol.* **100**, 1897–1908.
Xu JH, Long L, Tang YC, Hu HT, Tang FR (2007) Ca(v)1.2, Ca(v)1.3, and Ca(v)2.1 in the mouse hippocampus during and after pilocarpine-induced status epilepticus. *Hippocampus* **17**, 235–251.

Supporting Information

Additional Supporting Information may be found in the online version of this article at the publisher's web-site.

Fig. S1 Depiction of Immunoblots from CNC1 and ab144 antibody specificity on hippocampal and cerebellar tissue lysates.

Fig. S2 Examples depicting full length Immunoblots from Western blot analyses.

Fig. S3 Selective isolation of surface-expressed proteins.

Fig. S4 Examples depicting qRT-PCR amplification plots for $Ca_v1.2$ and $Ca_v1.3$ gene expression analyses.

Fig. S5 Regional expression of $Ca_v1.2$ and $Ca_v1.3$ L-type calcium channel proteins in dorsal hippocampus.